Chemical Science

EDGE ARTICLE

Check for updates

All publication charges for this article have been paid for by the Royal Society of Chemistry

Controlling the thermodynamic stability of conformational isomers of bistricyclic aromatic enes by introducing boron and silicon atoms†

Kohei Yamada,[a] Yohei Adachi ✩*[a] and Joji Ohshita ✩*[ab]

Overcrowded bistricyclic aromatic enes (BAEs) have several conformational isomers, including twisted and *anti*-folded conformers. These compounds change color depending on their conformation because each isomer exhibits distinct absorption bands. In this study, we introduced several heteroatoms such as boron and silicon into BAEs to control the energy difference between the twisted and *anti*-folded conformers, thereby achieving chromic properties. The heteroatom-containing BAEs showed absorption bands attributable to both twisted and *anti*-folded conformers, suggesting the coexistence of these conformers in solution. Although the solution appeared bluish, yellowish crystals were obtained by recrystallization. Single-crystal X-ray diffraction analysis confirmed that the yellowish crystals existed in the *anti*-folded conformation. The color of these crystals changed from yellowish to bluish upon heating and grinding, demonstrating thermochromism and mechanochromism. In addition, when cyanide ions were added to the BAE solution, the color changed from bluish to colorless, indicating the chemochromic properties of the BAEs.

Introduction

Chromism is a reversible change in color in response to an external stimulus. Materials with chromic properties have attracted great interest in recent years for their potential applications in imaging,[1] sensors,[2] and memory devices.[3] Overcrowded bistricyclic aromatic enes (BAEs) have been investigated as representative examples of these materials.[4] Because of the steric hindrance in the fjord regions, BAEs have several conformational isomers, including twisted and *anti*-folded conformers (Fig. 1). Generally, the conformational isomers of BAEs are in equilibrium and can isomerize thermally even at room temperature. Twisted conformers exhibit a more red-shifted absorption band in the visible region than the corresponding *anti*-folded conformers, which is ascribed to the twisted central C=C double bond. Therefore, BAEs can be applied as stimulus-responsive materials with chromic properties *via* conformational isomerization. Bianthrone, the first BAE to exhibit chromism, showed a color change from yellowish to greenish in response to heat, light, and pressure.[5] Following
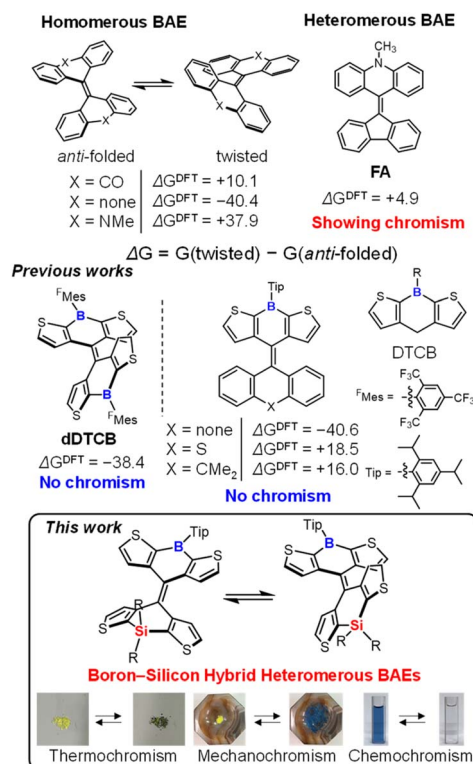
ᵃSmart Innovation Program, Graduate School of Advanced Science and Engineering, Hiroshima University, Higashi-Hiroshima, Hiroshima 739-8527, Japan. E-mail: yadachi@hiroshima-u.ac.jp; jo@hiroshima-u.ac.jp

ᵇDivision of Materials Model-Based Research, Digital Monozukuri (Manufacturing) Education and Research Center, Hiroshima University, Higashi-Hiroshima, Hiroshima 739-8527, Japan

† Electronic supplementary information (ESI) available. CCDC 2381482–2381484. For ESI and crystallographic data in CIF or other electronic format see DOI: https://doi.org/10.1039/d4sc06150k

Fig. 1 Structures of homomerous and heteromerous BAEs and their ΔG^{DFT} values in kJ mol^{-1} calculated by DFT at the B3LYP/6-31G(d) level. Calculation details are shown in Table S1.†

this finding, a variety of homomerous[5–7] and heteromerous[8–12] BAEs exhibiting chromism were reported. The energy difference between the twisted and *anti*-folded isomers (ΔG, defined as G(twisted) $- G$(*anti*-folded)) is an important factor controlling the isomerization of BAEs. Generally, $|\Delta G|$ should be small for BAEs to exhibit chromic properties,[4a,g,10] and this can be controlled by manipulating the flexibility of the tricyclic structures of BAEs. For example, bifluorenylidene, which is composed of rigid fluorene structures, exists only as a twisted conformer ($\Delta G^{DFT} = -40.4$ kJ mol^{-1}, Fig. 1 and Table S1†), whereas biacridinylidene, composed of flexible sp^3 nitrogen-bridged acridine structures, is only found in an *anti*-folded conformation ($\Delta G^{DFT} = +37.9$ kJ mol^{-1}, Fig. 1 and Table S1†). These compounds do not show any chromic behavior owing to their large $|\Delta G|$ values. As such, in order for BAEs to exhibit chromism, it is necessary to reduce the value of $|\Delta G|$ through specific molecular design. BAE structures that lead to chromism are quite limited, and indeed, for homomerous BAEs, only bianthrone[5a–c] and dixanthylene[6a] are known as thermochromic BAEs. For heteromerous BAEs, the combination of rigid and flexible tricyclic structures reduces $|\Delta G|$ (*e.g.*, fluorenylidene-acridane BAE (**FA**), $\Delta G^{DFT} = +4.9$ kJ mol; Fig. 1 and Table S1†), thereby achieving mechanochromism and thermochromism.[10] However, availability of conventional tricyclic structures is limited, and only a few examples of chromic BAEs combining a rigid fluorene unit and a more flexible anthrone,[8] xanthene,[9] acridane,[10] or thioxanthene[11] unit, or an anthrone unit and a xanthene unit,[12] have been reported. Therefore, the development of tricyclic structures for use in the construction of BAE systems is crucial for advancing new chromic BAEs.

Boron- and silicon-containing organic materials exhibiting different properties from conventional carbon-based materials have attracted recent attention. For example, conjugated tri-coordinate boron compounds are characterized by the presence of an empty 2p orbital on the boron atom. The empty 2p orbital interacts with neighboring π^* orbitals, thereby effectively stabilizing the LUMO level.[13] Furthermore, π-conjugated tri-coordinate boron compounds can form complexes with Lewis bases, making them applicable to anion-responsive sensor materials.[14] Silicon is also an interesting group 14 heavy element. It is widely known that the σ^* orbital of the Si–C bond interacts with the π^* orbital, lowering the LUMO level of the compound.[15] These features highlight the importance of using heteroatoms to develop new functional materials. We have previously reported the synthesis of **dDTCB** as a homomerous BAE with two tricoordinate boron atoms (Fig. 1).[16] The introduction of a rigid tricoordinate boron unit into the thiophene-based BAE greatly stabilized the twisted conformation ($\Delta G^{DFT} = -38.4$ kJ mol^{-1}, Fig. 1 and Table S1†), resulting in the observation of only the twisted conformer both in solution and as a solid. Although **dDTCB** did not show chromism because of its large $|\Delta G|$, it clearly suggested the potential of using heteroatoms to control ΔG. We have also reported the development of heteromerous BAEs based on the DTCB structure with fluorene, thioxanthene, and 9,10-dihydroanthracene (Fig. 1).[17] As mentioned above, however, the precise control of ΔG was quite difficult when combining conventional tricyclic

structures, and the heteromerous DTCB-based BAEs failed to achieve mechanochromic and thermochromic properties. Thus, to develop new chromic BAEs, we focused on the use of heteroatoms as a new method to precisely control ΔG of BAEs, rather than relying on conventional tricyclic structures. We replaced one of the boron atoms with a silicon atom in **dDTCB** (which was found to predominantly exist in the twisted conformation because of the rigid tricyclic structure), expecting that the rigidity of the DTCB tricyclic structure would be balanced by the flexible Si–C bond, thus causing a decrease in $|\Delta G|$. Indeed, the synthesized boron–silicon hybrid hetero-merous BAEs had very small $|\Delta G|$ values, leading to the development of new mechanochromic and thermochromic BAEs. Furthermore, the isomerization of BAEs was induced by the coordination of Lewis bases to boron in titration experiments, indicating that the introduction of heteroatoms can impart new functionalities such as chemochromism to BAEs.

Results and discussion

DFT calculation

To investigate in detail how introducing heteroatoms affects the thermodynamic stability of the conformational isomers of BAEs, we first performed DFT calculations on the three model compounds: sp^2 boron-containing **dDTCB′**, with a 2,4,6-triiso-propylphenyl (Tip) group replacing the ^{F}Mes group on the boron atom of **dDTCB**; **dDTCC** having two sp^3 carbon atoms; and **dDTCSi** having two sp^3 silicon atoms (Fig. 2a and S1†). Consistent with a previous report,[17] the twisted conformer of
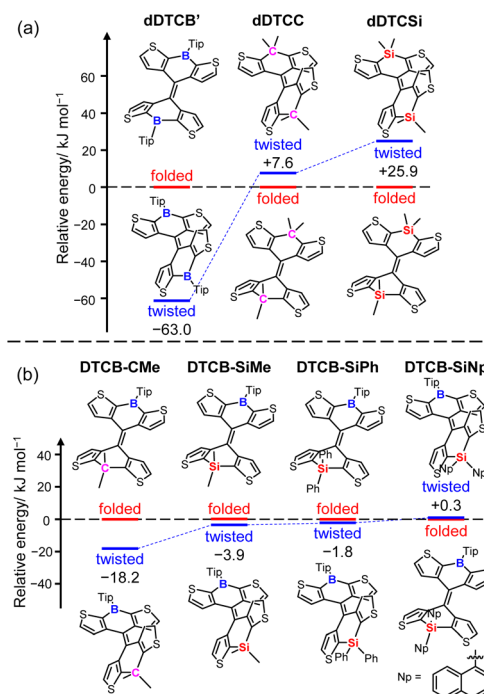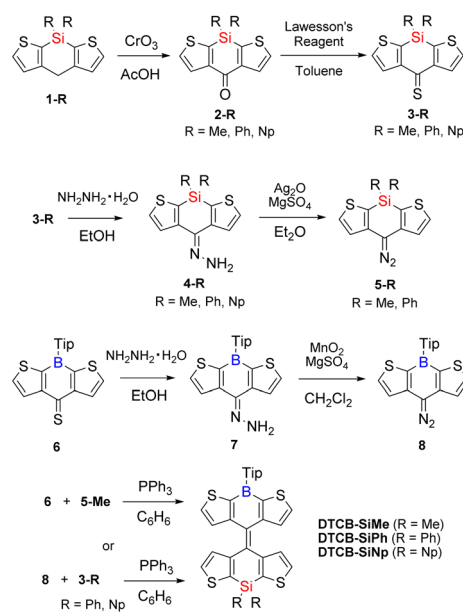

Fig. 2 DFT-calculated relative Gibbs energy diagram of thiophene-based (a) homomerous and (b) heteromerous BAEs at the B3LYP/6-31G(d) level at 298 K. The energy of the corresponding *anti*-folded conformer is set as zero.

dDTCB′ is more stable than its *anti*-folded counterpart, with a ΔG^{DFT} of −63.0 kJ mol^{-1}. In contrast, the twisted conformer of **dDTCC** is greatly destabilized, with the *anti*-folded conformer being more stable (ΔG^{DFT} = +7.6 kJ mol^{-1}). The *anti*-folded conformer of **dDTCSi** is even more stable (ΔG^{DFT} = +25.9 kJ mol^{-1}). These results demonstrate that replacing rigid sp^2 boron atoms with sp^3 carbon and silicon atoms significantly stabilizes the *anti*-folded conformation relative to the corresponding twisted conformation. The greater stabilization of the *anti*-folded conformer of **dDTCSi** compared with that of **dDTCC** is likely due to the longer Si–C bond compared with the C–C bond (Table S2†), which makes the tricyclic structure more flexible. On the basis of these calculations, we expected that combining boron- and carbon/silicon-containing tricyclic systems could achieve BAEs with small $|\Delta G|$ values, and performed calculations for **DTCB-CMe** and **DTCB-SiMe** (Fig. 2b and S2†). In the twisted conformers of these heteromerous BAEs, the tricyclic structures are highly planar (**DTCB-CMe:** A–B = 2.5°, C–D = 0.8°; **DTCB-SiMe:** A–B = 1.9°, C–D = 6.2°; Table S3†) and highly twisted around the central C=C double bond (**DTCB-CMe:** ω = 46.7°, **DTCB-SiMe:** ω = 49.3°). On the other hand, in the *anti*-folded conformers, the tricyclic structures are not planar, and those with a carbon or silicon bridging atom are bent to a greater extent than those with the boron-bridged DTCB unit (**DTCB-CMe:** A–B = 32.1°, C–D = 49.0°; **DTCB-SiMe:** A–B = 29.9°, C–D = 58.8°). The central C=C double bonds are longer in the twisted conformers than in the *anti*-folded conformers (Table S3†), consistent with a previous report.[17] The calculated ΔG^{DFT} values of **DTCB-CMe** and **DTCB-SiMe** are −18.2 and −3.9 kJ mol^{-1}, respectively (Fig. 2b). As expected, the ΔG^{DFT} values of these heteromerous BAEs are between the ΔG^{DFT} values of the corresponding homomerous BAEs. Notably, **DTCB-SiMe**, a boron–silicon hybrid BAE, has a very small $|\Delta G^{DFT}|$. To investigate the influence of substituents on the silicon atom, calculations were also performed for **DTCB-SiPh** and **DTCB-SiNp** with phenyl and naphthyl groups, respectively, instead of the methyl groups (Fig. 2b and S2†). The twisted conformer tended to become slightly less stable with increasing bulkiness of the substituents (Me < Ph < Np). The very small $|\Delta G^{DFT}|$ values of **DTCB-SiMe**, **DTCB-SiPh**, and **DTCB-SiNp** strongly suggest that these compounds exhibit chromism.

Synthesis

From the DFT calculations, we predicted that the boron–silicon hybrid BAEs have very small $|\Delta G|$ values. These heteromerous BAEs were synthesized from the corresponding diaryldiazomethanes and diarylthioketones *via* the Barton–Kellogg reaction (Scheme 1). Starting compounds **1-Me** and **6** were synthesized following the literatures,[16,17] and **1-Ph** and **1-Np** were synthesized using a similar procedure to that for **1-Me**. First, **1-Me**, **1-Ph**, and **1-Np** were oxidized by CrO$_3$ to give ketones **2-Me**, **2-Ph**, and **2-Np**, respectively. These ketones were then treated with Lawesson's reagent to give corresponding thioketones **3-Me**, **3-Ph**, and **3-Np**. Compound **3-Me** was treated with hydrazine monohydrate to afford hydrazone **4-Me**, and this was oxidized with Ag$_2$O to yield desired diazo compound **5-Me**.

Scheme 1 Synthetic route of boron- and silicon-containing BAEs *via* the Barton–Kellogg reaction.

Compound **5-Ph** could be synthesized using the same procedures, but it was found that **5-Ph** was sensitive to light and difficult to handle. Therefore, we switched the combination of the diazomethanes and thioketones for the Ph- and Np-substituted compounds. To synthesize boron-containing diazo compound **8**, hydrazone **7** was oxidized by MnO$_2$. Finally, Barton–Kellogg reactions were conducted using **5-Me** and **6** to afford **DTCB-SiMe**; **DTCB-SiPh** and **DTCB-SiNp** were obtained by the reactions of **8** with **3-Ph** and **3-Np**, respectively. The synthesized heteromerous BAEs were light bluish in solution but yellowish green in the solid state, as apparent upon solvent removal. These BAEs were stable in air and showed no decomposition even after storage for more than 6 months in the solid state. The chemical structures of them were confirmed by NMR and HR-mass spectrometry. The TG/DTA analysis of the synthesized BAEs showed increasing thermal stability with increasing bulkiness of the substituents on the silicon atom (Fig. S3†).

Optical properties

To gain insight into the conformers of the synthesized heteromerous BAEs, the UV-vis absorption spectra of **DTCB-SiMe**, **DTCB-SiPh**, and **DTCB-SiNp** in toluene were compared with that of **dDTCB′** (Fig. 3 and Table S4†). **DTCB-SiMe**, **DTCB-SiPh**, and **DTCB-SiNp** showed two absorption maxima around 400 and 600 nm. Generally, the absorption bands of twisted conformers are observed in the visible region,[5,8–10] suggesting that the absorption bands around 600 nm correspond to those of the twisted conformers of the heteromerous BAEs. The long-wavelength absorption maximum of **DTCB-SiMe** was slightly blue-shifted relative to that of **dDTCB′**, likely due to the reduced p–π* interaction in **DTCB-SiMe**. Notably, the long-wavelength absorption bands of the heteromerous BAEs were much weaker than that of the twisted conformer-predominant
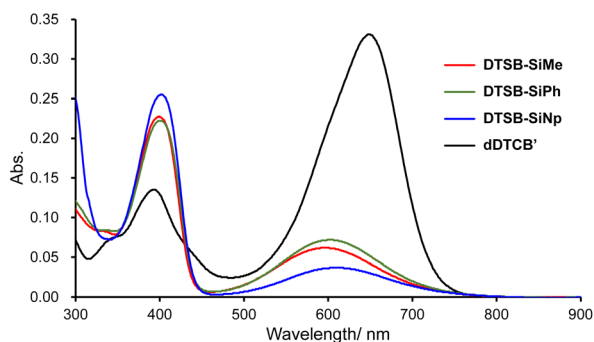
Fig. 3 UV-vis absorption spectra of DTCB-SiMe, DTCB-SiPh, DTCB-SiNp, and dDTCB′ in toluene at a concentration of 10 μmol L^{-1}.

dDTCB′, suggesting that the ratio of twisted conformers to *anti*-folded conformers in these heteromerous BAEs is much smaller than that in **dDTCB′**. On the other hand, the absorption bands around 400 nm, which are likely attributed to the absorption of the *anti*-folded conformers (*vide infra*), were much stronger for the heteromerous BAEs than **dDTCB′**. These results suggest that the twisted and *anti*-folded conformers of the heteromerous BAEs coexist in solution, as predicted from the small $|\Delta G^{DFT}|$ values derived from the DFT calculations. The long-wavelength absorption maximum of **FA**[10a] was observed at 680 nm, and even though the twist angle of the double bond in the twisted conformer of **DTCB-SiMe** ($\omega = 49.3°$, see Table S3†) was larger than that of **FA** ($\omega = 43.9°$),[10a] the long-wavelength absorption maximum of **DTCB-SiMe** was observed at a shorter wavelength (600 nm). This is considered to be due to the broken conjugation within the tricyclic structure because of bridging with the sp^3 silicon atom. The intensity of the absorption band around 600 nm decreased in the order of **DTCB-SiPh** ≈ **DTCB-SiMe** > **DTCB-SiNp**, suggesting that the substituents on the silicon atom slightly influence the thermodynamic stability of the conformational isomers. TD-DFT calculations were performed for the heteromerous BAEs to determine electronic transitions in the UV-vis absorption spectra (Fig. S4–S7, Tables S5–S10†). The absorption bands around 600 nm were in good agreement with the HOMO → LUMO transition of the twisted conformers, whereas the absorption bands around 400 nm were consistent with the HOMO → LUMO transition of the *anti*-folded conformers and larger energy transitions in the twisted conformers (Fig. S5–S7†). These TD-DFT calculations strongly support the coexistence of the twisted and *anti*-folded conformers of the heteromerous BAEs in solution. The photoluminescence (PL) spectrum of **DTCB-SiMe** showed an emission at 470 nm upon excitation at 399 nm (Fig. S8†). On the other hand, no PL was observed when excitation was performed at 596 nm, which is in line with the general trend of twisted conformers not exhibiting PL, as opposed to the *anti*-folded conformers.[10a,16] The PL maxima of **DTCB-SiPh** and **DTCB-SiNp** were almost identical to that of **DTCB-SiMe**, suggesting the negligible effect of the silicon substituents on the photoexcited state of the *anti*-folded conformers.

Next, cyclic voltammetry was performed in CH$_2$Cl$_2$ containing 0.1 M Bu$_4$NPF$_6$ at a scan rate of 100 mV s^{-1}. The cyclic voltammograms of the heteromerous BAEs showed two irreversible oxidation waves and two irreversible reduction waves (Fig. S9 and S10 and Table S11†). The HOMO–LUMO energy gaps estimated from the first oxidation and reduction potentials were 1.74, 1.64, and 1.70 eV for **DTCB-SiMe**, **DTCB-SiPh**, and **DTCB-SiNp**, respectively. These values roughly matched the HOMO–LUMO gaps estimated from the absorption edges in toluene (Table S11†), indicating that the first oxidation and reduction waves were derived from the twisted conformers. Compared with **FA**,[10a] both the HOMO and LUMO levels were low in **DTCB-SiMe**, which could be explained by the electron-donating nitrogen in **FA** and the electron-withdrawing boron in **DTCB-SiMe**.

NMR analysis

Next, to investigate the thermodynamic properties of the heteromerous BAEs in solution, variable-temperature (VT) ^{1}H NMR spectra of **DTCB-SiPh** were measured (Fig. 4 and S11†). In the room-temperature ^{1}H NMR spectrum, the signals corresponding to each conformer were not observed separately, and some peaks were broadened. This suggests that the twisted and *anti*-folded conformers interconvert rapidly at room temperature. Upon cooling the solution, the signals gradually broadened further, and at around −40 °C, the signals corresponding to each conformer appeared separately. A van't Hoff plot was obtained from the signals corresponding to the isopropyl groups on the Tip group, as shown in Fig. 4. Changes in enthalpy (ΔH) and entropy (ΔS) between the *anti*-folded and twisted conformers were found to be +1.16 kJ mol^{-1} and −15.4 J (mol^{-1} K^{-1}), respectively (Fig. 4). The ΔG value at 298 K was calculated to be +3.43 kJ mol^{-1}, indicating that the *anti*-folded conformer is slightly more stable. This ΔG value of **DTCB-SiPh** was similar to that of a derivative of **FA** ($\Delta G = +3.43$ kJ mol^{-1})[10c] but was inconsistent with the DFT results of **DTCB-SiPh** (Fig. 2, $\Delta G^{DFT} = -1.8$ kJ mol^{-1}), suggesting that the twisted conformer of **DTCB-SiPh** was slightly more stable than the *anti*-folded conformer. The VT-NMR results indicate that whereas DFT calculations are useful for estimating conformer stability, a certain degree of
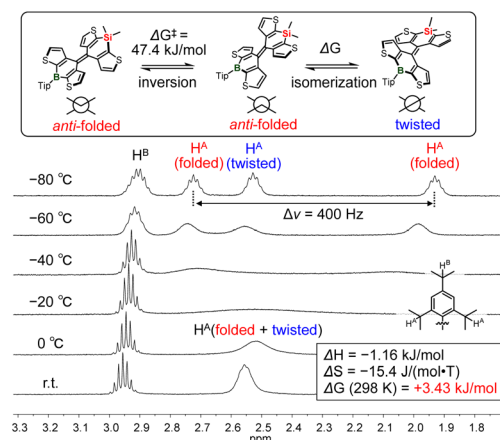

Fig. 4 Variable temperature ^{1}H NMR spectra of DTCB-SiPh in aliphatic region in CD$_2$Cl$_2$.

discrepancy exists between the calculated and experimentally determined ΔG. To obtain a more accurate ΔG by DFT calculations, further examination of functionals and other factors is necessary. Nonetheless, the $|\Delta G|$ value of **DTCB-SiPh** estimated from the VT-NMR spectra is sufficiently small to suggest that **DTCB-SiPh** exhibits thermo/mechanochromism. The energy barrier ($\Delta G^{\ddagger}$) for the inversion of the *anti*-folded conformer was determined to be 47.4 kJ mol^{-1} (see ESI† for details), strongly supporting that **DTCB-SiPh** easily isomerizes at room temperature and is in thermal equilibrium. Although the $\Delta G^{\ddagger}$ value between the *anti*-folded and twisted conformers could not be determined, it is expected to be similar to the small value for the inversion of the *anti*-folded conformer because they are in thermal equilibrium at room temperature. Other signals of the aliphatic protons on the Tip group corresponding to each conformational isomer were also separately observed at low temperatures. However, the signals of the aromatic region were complex and poorly resolved.

Single-crystal X-ray diffraction analysis

In contrast to the heteromerous BAEs that appeared bluish in solution, yellowish-green solids were obtained after solvent removal (*vide supra*). To gain insight into the conformers in the solid state, single-crystal X-ray diffraction analysis was performed. Single crystals were obtained by slow evaporation of the solvent in a hexane solution of **DTCB-SiMe** and CH$_2$Cl$_2$/hexane solutions of **DTCB-SiPh** and **DTCB-SiNp**. All the recrystallized solids were yellow. The crystal structures confirmed that the heteromerous BAEs adopted the *anti*-folded conformation
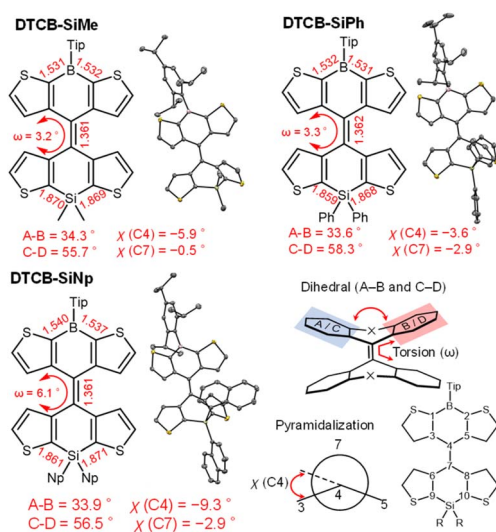

Fig. 5 Crystal structures of **DTCB-SiMe**, **DTCB-SiPh**, and **DTCB-SiNp** obtained at 100 K. Thermal ellipsoids are at the 50% probability level. Hydrogen atoms are omitted for clarity. Dihedral angle between the two mean planes (A–B and C–D) is defined as the dihedral angle between the least-square planes of the atoms in the thiophene rings of each tricyclic structure. Pyramidalization angles are defined as the improper torsion angles $\chi(C4) = [(\tau C3{-}C4{-}C7{-}C5)]$ MOD 360° minus 180° and $\chi(C7) = [\tau(C6{-}C4{-}C7{-}C8)]$ MOD 360° minus 180°. Torsion angle (ω) around C4=C7 is defined as the absolute value of average of the dihedral angles (τC3–C4–C7–C6) and τ(C5–C4–C7–C8).

(Fig. 5 and Table S12†). This finding is notable because both twisted and *anti*-folded conformers were observed in solution. The crystal structures are in good agreement with the DFT-optimized structures of the *anti*-folded conformers of the heteromerous BAEs. Other recrystallization solvents such as CH$_2$Cl$_2$/methanol and CH$_2$Cl$_2$/acetonitrile were also tested, however, no crystals of the twisted conformers were obtained.

Chromic properties

We investigated thermochromism and mechanochromism in the recrystallized solids. When the crystals of **DTCB-SiMe** were heated, the color changed from yellowish to bluish, indicating partial isomerization of the *anti*-folded conformer into the twisted conformer (Fig. 6a). Upon cooling to room temperature, the color changed back to yellowish, suggesting reversible isomerization. Next, mechanochromism was examined by grinding the crystals. The color of the crystals immediately changed from yellowish to bluish (Fig. 6b), and the ground bluish solid turned greenish upon exposure to CH$_2$Cl$_2$ vapor, suggesting partial recovery of the *anti*-folded conformation. The blue color of the ground solid could be also recovered to yellowish by thermal annealing (Fig. 6b). Similar thermochromism and mechanochromism were also observed for **DTCB-SiPh** (Fig. S13 and S14†). For **DTCB-SiNp**, the color did not completely recover after cooling or exposure to CH$_2$Cl$_2$ vapor (Fig. S13†), suggesting that the substituents on the silicon atom influence the reversibility of the chromism. Matsuo *et al.* reported obtaining yellowish solids of pure *anti*-folded conformers of **FA** by precipitation through sonication in methanol or ethanol,[10] which is a much easier procedure for obtaining *anti*-folded solids than recrystallization. The application of similar sonication to the boron–silicon hybrid heteromerous BAEs produced yellowish precipitates of *anti*-folded conformers, and they also exhibited thermo/mechanochromism (Fig. S15†). In the UV-vis absorption spectrum of the initial yellowish solid, the absorption band around 600 nm was not observed; however, it was significantly increased after grinding (Fig. S16†). Exposure to CH$_2$Cl$_2$ vapor
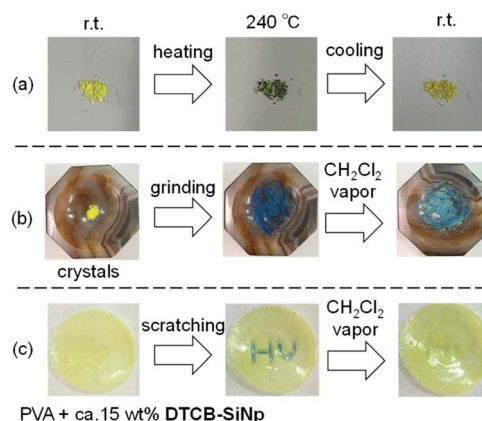

Fig. 6 (a) Thermochromic and (b) mechanochromic properties of crystals of **DTCB-SiMe**. (c) Mechanochromism of the PVA film with **DTCB-SiNp**.

reduced the intensity of the absorption band around 600 nm, suggesting that the *anti*-folded conformation was partially recovered. The powder X-ray diffraction pattern of the solid precipitated from methanol did not match the pattern simulated from the single-crystal X-ray data; however, its sharp signals suggested the crystalline nature of the precipitate (Fig. S17†). After grinding, the peak intensities decreased, and a weak diffraction pattern similar to that of the single crystal was observed. This suggests that through grinding, some of the crystalline phase of the precipitated solid became amorphous, and the remainder transitioned into the crystal phase observed in the single-crystal X-ray diffraction analysis. Because of the small $|\Delta G|$ of the heteromerous BAEs, the amorphous phase partially underwent isomerization into the twisted conformer, resulting in a change in color of the solid from yellowish to bluish. After exposure to CH_2Cl_2 vapor or heating, the intensity of the diffraction peaks of the crystals increased, indicating partial conversion of the twisted conformer in the amorphous phase into the *anti*-folded conformer. The appearance of these thermo/mechanochromic behaviors is attributed to the small $|\Delta G|$ values of the heteromerous BAEs, demonstrating that the use of heteroatoms to control ΔG is an effective approach. Inspired by the application of BAEs by Matsuo *et al.*,[10d–f] **DTCB-SiNp** in the solid state was dispersed in the polyvinyl alcohol (PVA) film to investigate its mechanochromic properties (Fig. 6c). The as-prepared PVA film was yellowish, but the scratched area become blueish. Exposing this film to CH_2Cl_2 vapor completely restored the scratched area to yellow, and this process could be repeated.

Titration experiments

Because the heteromerous BAEs have a tricoordinate boron, a titration experiment was performed with **DTCB-SiPh** using tetrabutylammonium cyanide (TBACN) (Fig. 7). When TBACN was added to a toluene solution of **DTCB-SiPh**, the color of the solution changed from bluish to colorless. In the UV-vis absorption spectra, the original absorption bands around 600 nm and 400 nm gradually decreased, and a new absorption band appeared around 350 nm. The presence of isosbestic points at 315 nm and 373 nm indicates that **DTCB-SiPh** and cyanide formed a complex without decomposition. The [11]B

NMR spectra revealed a peak shift from around 50 ppm in the absence of cyanide to −20 ppm after the addition of TBACN, confirming the formation of tetracoordinate boron species (Fig. S18†). The color of the solution changed back to bluish upon the addition of $BF_3 \cdot Et_2O$, a strong Lewis acid (Fig. S19†), suggesting that the boron center changed from tetracoordinate to tricoordinate. This drastic color change likely results from the shift in the thermal equilibrium between the twisted and *anti*-folded conformers. Upon complexation, the boron center changed from sp[2] to sp[3], making the tricyclic structure more flexible. Thus, the *anti*-folded conformer was stabilized in the presence of cyanide, and the color of the solution changed from bluish to colorless as the *anti*-folded conformer became predominant. Similar behaviors were observed for **DTCB-SiMe** and **DTCB-SiNp** toward the addition of TBACN (Fig. S20†). The ΔG^{DFT} values of **DTCB-SiPh** change from −1.8 kJ mol^{-1} to +3.5 kJ mol^{-1} upon the complexation with cyanide, revealing the stabilization of *anti*-folded conformer in the presence of cyanide (Table S13†). To further examine the selectivity of anions, UV-vis absorption spectral changes of the heteromerous BAEs were monitored before and after the addition of other anions including fluoride, chloride, and bromide (Fig. S21†). As similar to conventional tricoordinate boron compounds, these BAEs showed no response to chloride and bromide ions. For fluoride ions, **DTCB-SiPh** and **DTCB-SiNp** exhibited similar spectral changes as with cyanide ions (Fig. S21†). In the case of **DTCB-SiMe**, the solution turned yellow upon the addition of fluoride ions (Fig. S21†), suggesting that the silicon unit was hydrolyzed due to the smaller steric bulkiness of the substituents on the silicon atom (Fig. S22†). The heteromerous boron–silicon hybrid BAEs exhibited selective chemochromism toward anions owning to the Lewis acidity of the tricoordinate boron, demonstrating a very drastic color change compared with common tricoordinate boron compounds.[14]

Conclusions

In summary, we synthesized BAEs exhibiting various types of chromism by introducing heteroatoms. Using this new approach to control ΔG with heteroatoms, we discovered that boron–silicon hybrid heteromerous BAEs have very small $|\Delta G|$ values and exhibit both thermochromism and mechanochromism. By leveraging the specific reactivity of tricoordinate boron, we demonstrated the possibility of imparting new anion-induced chemochromism to BAEs. These results highlight the potential of using heteroatoms in the molecular design of stimulus-responsive BAEs.

Data availability

All data are available in the manuscript and in the ESI.†

Author contributions

Kohei Yamada: formal analysis; investigation; writing – original draft. Yohei Adachi: conceptualization; funding acquisition;
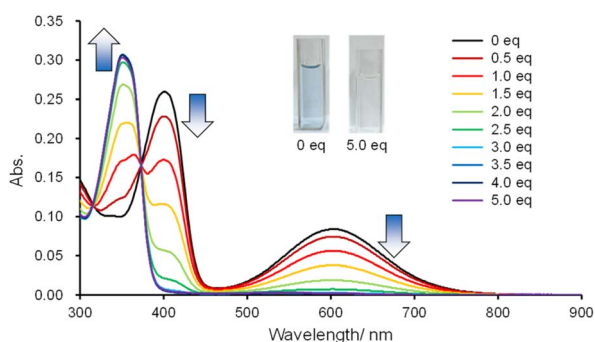

Fig. 7 Absorption data for titrations of **DTCB-SiPh** with TBACN aliquots in toluene at the concentration of 10 μmol L^{-1}.

Conflicts of interest

There are no conflicts to declare.

Acknowledgements

Notes and references

1 N. Bar and P. Chowdhury, *ACS Appl. Electron. Mater.*, 2022, **4**, 3749.

2 (a) Y. Chen, G. Mellot, D. van Luijk, C. Creton and R. P. Sijbesma, *Chem. Soc. Rev.*, 2021, **50**, 4100; (b) M. Bayat, H. Mardani, H. Roghani-Mamaqani and R. Hoogenboom, *Chem. Soc. Rev.*, 2024, **53**, 4045.

3 M. Irie, T. Fukaminat, K. Matsud and S. Kobatake, *Chem. Rev.*, 2014, **114**, 12174.

4 (a) P. U. Biedermann, J. J. Stezowski and I. Agranat, *Eur. J. Org. Chem.*, 2001, 15; (b) P. U. Biedermann, J. J. Stezowski and I. Agranat, *Chem. Commun.*, 2001, 954; (c) A. Levy, S. Pogodim, S. Cohen and I. Agranat, *Eur. J. Org. Chem.*, 2007, 5198; (d) A. Takai, D. J. Freas, T. Suzuki, M. Sugimoto, J. Labuta, R. Haruki, R. Kumai, S. Adachi, H. Sakai, T. Hasobe, Y. Matsushita and M. Takeuchi, *Org. Chem. Front.*, 2017, **4**, 650; (e) P. U. Biedermann, J. J. Stezowski and I. Agranat, *Chem.–Eur. J.*, 2006, **12**, 3345; (f) Y. Hirao, N. Nagamachi, K. Hosoi and T. Kubo, *Chem.–Asian J.*, 2018, **13**, 510; (g) Y. Hirao, Y. Hamamoto and T. Kubo, *Chem.–Asian J.*, 2022, **17**, e202200121; (h) H. Tanaka, Y. Mizuhata, N. Tokitoh, R. Miyamoto, K. Kanamori and H. Kaji, *J. Phys. Chem. C*, 2023, **127**, 20459.

5 (a) W. T. Grubb and G. B. Kistiakowsky, *J. Am. Chem. Soc.*, 1950, **72**, 419; (b) Z. R. Grabowski and M. S. Balasiewicz, *Trans. Faraday Soc.*, 1968, **64**, 3346; (c) Y. Tapuhi, O. Kalisky and I. Agranat, *J. Org. Chem.*, 1979, **44**, 1949; (d) H. Meyer, *Ber. Dtsch. Chem. Ges. B*, 1909, **42**, 143; (e) H. Meyer, *Monatsh. Chem.*, 1909, **30**, 165; (f) D. L. Fanselow and H. G. Drickamer, *J. Chem. Phys.*, 1974, **61**, 4567; (g) Y. Hirshberg and E. Fischer, *J. Chem. Soc.*, 1953, 629; (h) R. S. Becker and C. E. Earhart, *J. Am. Chem. Soc.*, 1970, **92**, 5049; (i) E. Fischer, *Rev. Chem. Intermed.*, 1984, **5**, 393.

6 (a) A. Schönberg, A. Mustafa and M. E. E.-D. Sobhy, *J. Am. Chem. Soc.*, 1953, **75**, 3377; (b) R. Korenstein, K. A. Muszkat and E. J. Fischer, *Photochem*, 1976, **5**, 447; (c) M. Hoshino, M. Matsui and M. Imamura, *Bull. Chem. Soc. Jpn.*, 1974, **47**, 534.

7 (a) W. R. Browne, M. M. Pollard, B. de Lange, A. Meetsma and B. L. Feringa, *J. Am. Chem. Soc.*, 2006, **128**, 12412; (b) O. Ivashenko, H. Logtenberg, J. Areephong, A. C. Coleman, P. V. Wesenhagen, E. M. Geertsema, N. Heureux, B. L. Feringa, P. Rudolf and W. R. Browne, *J. Phys. Chem. C*, 2011, **115**, 22965; (c) B. P. Corbet, M. B. S. Wonink and B. L. Feringa, *Chem. Commun.*, 2021, **57**, 7665.

8 A. Levy, S. Pogodim, S. Cohen and I. Agranat, *Eur. J. Org. Chem.*, 2007, 5198.

9 H. Takezawa, T. Murase and M. Fujita, *J. Am. Chem. Soc.*, 2012, **134**, 17420.

10 (a) T. Suzuki, H. Okada, T. Nakagawa, K. Komatsu, C. Fujimoto, H. Kagi and Y. Matsuo, *Chem. Sci.*, 2018, **9**, 475; (b) Y. Matsuo, Y. Wang, H. Ueno, T. Nakagawa and H. Okada, *Angew. Chem., Int. Ed. Engl.*, 2019, **58**, 8762; (c) Y. Wang, Y. Ma, K. Ogumi, B. Wang, T. Nakagawa, Y. Fu and Y. Matsuo, *Commun. Chem.*, 2020, **3**, 93; (d) K. Ogumi, K. Nagata, Y. Takimoto, K. Mishiba and Y. Matsuo, *J. Mater. Chem. C*, 2022, **10**, 11181; (e) K. Ogumi, K. Nagata, Y. Takimoto, K. Mishiba and Y. Matsuo, *Sci. Rep.*, 2022, **12**, 16997; (f) K. Ogumi, T. Arakawa, B. Okudera, Y. Takimoto, K. Nagata, K. Mishiba, E. Abe, T. Ueno, J. Hieda, K. Omote, H. S. Lin and Y. Matsuo, *ACS Appl. Eng. Mater.*, 2024, **2**, 397.

11 A. Schönberg and M. M. Sidky, *J. Am. Chem. Soc.*, 1959, 2259.

12 A. Schönberg, A. F. A. Ismail and W. Asker, *J. Chem. Soc.*, 1946, 442.

13 (a) A. Wakamiya and S. Yamaguchi, *Bull. Chem. Soc. Jpn.*, 2015, **88**, 1357; (b) Y. Ren and F. Jäkle, *Dalton Trans.*, 2016, **45**, 13996; (c) E. von Grotthuss, A. John, T. Kaese and M. Wagner, *Asian J. Org. Chem.*, 2018, **7**, 37; (d) M. Hirai, N. Tanaka, M. Sakai and S. Yamaguchi, *Chem. Rev.*, 2019, **119**, 8291; (e) X. Yin, J. Liu and F. Jäkle, *Chem.–Eur. J.*, 2021, **27**, 297.

14 (a) S. Yamaguchi, S. Akiyama and K. Tamao, *J. Am. Chem. Soc.*, 2001, **123**, 11372; (b) H. Li, R. A. Lalancette and F. Jäkle, *Chem. Commun.*, 2011, **47**, 9378; (c) K. Hu, Z. Zhang, J. Burke and Y. Qin, *J. Am. Chem. Soc.*, 2017, **139**, 11004; (d) A. Lik, S. Jenthra, L. Fritze, L. Müller, K.-N. Truong and H. Helten, *Chem.–Eur. J.*, 2018, **24**, 11961; (e) Y. Adachi, K. Yamada and J. Ohshita, *Chem. Lett.*, 2022, **51**, 654; (f) Y. Adachi, F. Arai, M. Sakabe and J. Ohshita, *Polym. Chem.*, 2021, **12**, 3471.

15 (a) J. Ohshita, K. Kimura, K.-H. Lee, A. Kunai, Y.-W. Kwak, E.-C. Son and Y. Kunugi, *J. Polym. Sci., Part A: Polym. Chem.*, 2007, **45**, 4588; (b) J. Ohshita, *Macromol. Chem. Phys.*, 2009, **210**, 1360; (c) T. Matsumoto, K. Tanaka and Y. Chujo, *RSC Adv.*, 2015, **5**, 55406; (d) H. Bin, L. Gao, Z.-G. Zhang, Y. Yang, Y. Zhang, C. Zhang, S. Chen, L. Xue, C. Yang, M. Xiao and Y. Li, *Nat. Commun.*, 2016, 7, 13651.

16 Y. Adachi, T. Nomura, S. Tazuhara, H. Naito and J. Ohshita, *Chem. Commun.*, 2021, **57**, 1316.

17 K. Yamada, Y. Adachi and J. Ohshita, *Chem.–Eur. J.*, 2023, **29**, e202302370.